Removal of malachite green dye from aqueous solution through inexpensive and easily available tuffite, bentonite and vitreous tuff minerals

A. Blanco-Flores[1,2], E. Gutiérrez-Segura[*], V. Sánchez-Mendieta[1], A. R. Vilchis-Néstor[3]

[1] *Facultad de Química, Universidad Autónoma del Estado de México. Toluca, Estado de México. México.*
[2] *División de Ingeniería Mecánica, Tecnológico de Estudios Superiores de Tianguistenco, Tianguistenco, Estado de México, México.*
[3] *Centro Conjunto de Investigación en Química Sustentable UAEM-UNAM, Toluca, Estado de México. México.*

Abstract

Tuffite (TUF), bentonite (BEN) and vitreous tuff (VT) accessible minerals were investigated as malachite green dye adsorbent materials. The morphology, textural and structural properties of the minerals were investigated by Scanning Electron Microscopy, Infrared Spectroscopy, X-Ray Diffraction, specific surface area (SBET), pH at zero charge, and chemical composition. The equilibrium times for BEN, TUF and VT minerals were 55 min, 80 min and 60 min, respectively. The best fit was achieved with a pseudo second-order model which may indicate that the adsorption process is dominated by chemisorption. The mechanism of adsorption was better described by film and intraparticle diffusion process. The adsorption capacities of dye onto VT, BEN and TUF were 71.22, 84.90 and 212.75 mg g^{-1}. In a comparative study, the amount removal for acid green 25 dye were 130.30 mg g^{-1}, 119.56 mg g^{-1} and 25.43 mg g^{-1}, respectively. The removal of dyes occurred through a combination of mechanisms. The adsorption behavior in a fixed-bed system was better described by Bohart-Adams and Thomas model for Co=50 mg l^{-1} Co=100 mg l^{-1} respectively. TUF mineral could be employed as a very effective adsorbent for dyes removal002E.

Key words: Tuffite, bentonite, vitreous tuff, malachite green, batch and column adsorption.

*Autores de correspondencia
Email: blancoflores81@hotmail.com. Tel-fax: 52 722-2173890

Introduction

Textile industry is considered as one of the most pollutant, due of the presence of organic toxic compounds known as dyes. Their presence in water reduces light penetration, blocking the occurrence of photosynthesis of aqueous flora. They are certainly not aesthetically, cause allergy, skin irritation and can provoke cancer and mutation in humans (Han *et al*., 2015).

Cationic dyes act as bases and when made soluble in water, they form a colored cationic salt, which can react with the anionic sites on the surface of the substrate (Gupta, 2009) these dyes are more toxic than anionic dyes, and they are resistant to degradation for biological methods (El-Sayed, 2011).

Malachite green is a basic dye, readily soluble in water. It is highly effective against important protozoan and fungal infections of fish and specifically in salmonids farming, most frequently used as disinfectant. It is used as a food-coloring agent, food additive, an anthelminthic as well as a dye in textile, paper and acrylic industries. In México this dye is also used for staining herbicides, and the wastewater resulted from herbicide synthesis process is colored with this dye. The basic chemical structure of malachite green and its metabolites indicates certain degree of carcinogenicity. Malachite green is transformed in organisms to leucomalachite green, which accumulates in the tissues of exposed organisms from where it can easily get into the human food chain (Gopinathan *et al*., 2015).

Acid dyes, also known as acid anthraquinone are difficult to remove; they contain anionic compounds, and are stable in water. They are used for dyeing fabrics like polyamide, acryl and silk, presents in hair dye formulation and cosmetics products. For these reasons the presence of these dyes in water could compromise the quality of the environment. Acid green 25 in particular belongs to an acid type dye and may affect the health of aquatic organism and safety of consumers of these types of organisms when wastewater is discharged on other water sources.

Among the advanced chemical or physical treatments of dye removal, adsorption is considered more effective and less expensive than other technologies such as ozone or electrochemical oxidation. The batch and column adsorption has been extensively studied for dye removal. Although the column system is effective and common for wastewater treatment, the batch system allows determining the maximum adsorption capacity (Himanshu and Vashi, 2012).

Many efforts have been made to investigate the development of adsorbent materials. However, from the economic and commercial points of view, this process has some disadvantages for scale up applications, using, therefore, common but until some extent expensive adsorbent materials, such as activated carbon. For this reason, cheap, available and disposable materials, with high removal efficiency, and without needing regeneration are highly demanded nowadays. Some of these adsorbent materials could be developed using natural minerals, whose interest to environmental applications is increasing every day.

Actually the dye removal process combines several processes such as: adsorption, exchange, precipitation and neutralization using different amount of chemical reagent and generated sludge waste. In nature there are minerals whose main phase is calcium carbonate. These minerals are able to carry out adsorption, precipitation and neutralization processes in wastewater treatment, simultaneously. Advantageously, they do not generate sludge and at the same time they can eliminate large amounts of toxic organic compounds (Xianming *et al*., 2012).

TUF mineral deposits are calcium carbonate-rich. $CaCO_3$ precipitation in tuffite produces a vast array of crystal forms; calcite predominates in most instances, followed by aragonite, and to a lesser extent $MgCO_3$. The SiO_2 and MgO are the next most abundant compounds and minor levels of Al_2O_3 and Fe_2O_3 are also found. The study of tuffites can benefit constraining models of climate change and paleo-hydrological reconstructions (McBride *et al*., 2012). This mineral has not been used as adsorbent material and has properties that can be important for removal of large amounts of organic compounds like dyes.

BEN is a clay mineral that contains montmorillonite mainly, with SiO_2, Al_2O_3, CaO, MgO, Fe_2O_3, Na_2O, K_2O as the main components. It has a high adsorption capacity because its structure is lamellar, which allows the absorption of some organic pollutants. This clay also provides an exchange ionic property between inorganic cations ($Na+$, Ca_2+, $K+$, Fe_3+) present in its structure and organic

ions (Arellano-Cárdenas *et al*., 2013).

The VT is related to other siliceous volcanic rocks, these rocks are named worldwide as volcanic glass and there are many types of these, like perlite and obsidian, whose origins and physic-chemical characteristics are similar among them (Qian *et al*., 2010). All these have high silica content (~70 %), are inexpensive and easily available in many countries. There are only a limited number of published papers on the use of perlite in the literature and the majority of these are about the use of expanded perlite like adsorbent material (Sarı *et al*., 2009). According to Qiangshan Jing *et al*., (2011 the expanded perlite is obtained by thermal treatment (800-1100 °C) which provokes the increase the porosity, but this procedure requires high temperature resulting in increased cost of production. Vitreous tuff main uses are directed to production of construction materials such as cements and concrete, soil improvement, laundry detergent, soil support and filling material. For these reasons, the vitreous tuff has a little economic value. There are different deposits and manifestations of vitreous tuff located in many countries that present volcanic origins, it has different surface properties and have been little studied towards environmental applications. Based upon its physical and chemical properties it has high potentialities for the treatment of liquid and gaseous waste, drinking water treatment and filtering of water for human consumption (Qian *et al*., 2010). The use as adsorbent material would add major economic value to these minerals and, most importantly, would provide a potentially inexpensive alternative to replace the use of expanded perlite as superior adsorbent material according to sorption characteristics.

In this work, tuffite, bentonite and vitreous tuff minerals were characterized by several techniques to obtain their morphological, textural and structural characteristics. In addition, their potential uses as basic-dye adsorbent materials, through kinetic and adsorption batch studies, were evaluated. Besides, the influence of structure of two dyes was analyzed on batch adsorption process from aqueous solutions for the three minerals. The best adsorbent mineral was then used to study its effectiveness for organic-dye removal in a column system.

Materials and methods

Adsorbent materials

BEN was obtained from Managua deposit located in Mayabeque. TUF was obtained from Samá Arriba deposit, Holguín and the VT comes from Magueyal deposit, Santiago de Cuba, Cuba. All of them were milled and sieved; the grain size used in this work was minor to 60 mesh (0.25 mm). The materials were used without pretreatment for the removal of malachite green and 25 acid green dyes from aqueous solutions in a batch process.

Malachite green and acid green 25 dyes

Malachite green chloride (MG, $C_{23}H_{25}N_2$, M=329.46 g mol^{-1}, cationic and basic dye) and acid green 25 (AG, $C_{28}H_{22}N_2NaO_8S_2$, M=624.59 g/mol, anionic and acid dye) (Figure 1a and b, respectively) were purchased (Hycel, México) and used without further purification. Dye solutions were prepared by dissolving an appropriate amount of dye in distilled water to obtain a range of concentrations for successive dilutions corresponding to 30-120 mg l^{-1}. The MG and AG dyes concentrations in the solutions were determined using a UV/Vis Perking Elmer Lambda 10 ultraviolet–visible spectrophotometer to 622 nm and 632 nm, respectively, as maximum wavelengths.

Characterization of minerals

Scanning Electron Microscopy

Scanning electron microscopy (SEM) images of VT, BEN, TUF minerals and of the samples after malachite green adsorption were acquired in a JEOL JSM 6510 microscope.

Chemical composition

Mineralogical composition of the samples was determined by Inductively Coupled Plasma-Atomic Emission Spectrometry (ICP-OES), using a Spectroflame FTMO8 Spectrophotometer.

Infrared Spectroscopy

Infrared spectra in the region from 4000-400 cm^{-1}, with a resolution of 4 cm^{-1} and 32 scans, were recorded for the adsorbent before and after adsorption process, at room temperature, using a Bruker Tensor 27 FTIR ATR spectrophotometer.

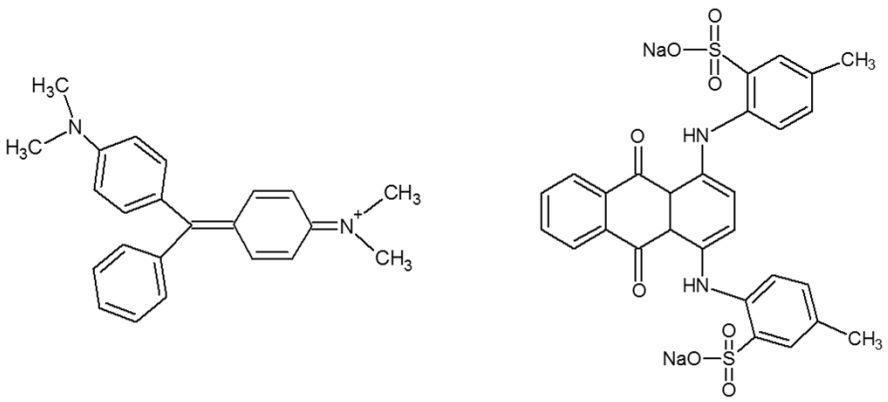

Figure 1. Chemical structures of malachite green (a) and acid green 25 (b) dyes.

X-Ray Diffraction

Crystalline phases present in minerals were analyzed on a Bruker D8 Advance diffractometer, using the CuKα (1.5406 Å) radiation line with nickel filter. The diffractograms were recorded from 5° to 80° (2θ) with a scan speed of 0.05°/s and a power tube of 30 KW. Identification of crystalline phases was carried out using the X'Pert High Score program.

Specific Surface Area (S_{BET})

Textural properties measurements were performed by using the nitrogen physisorption technique at 77 K in a Quantachrome Autosorb^{-1}. The specific surface areas were determined by the Brunnauer-Emmet-Teller (BET) equation. The adsorption-desorption isotherms were obtained by plotting the adsorbed volume of nitrogen under standard conditions of temperature and pressure (STP) versus the relative pressure P/Po to determine the pore size and estimate the shape of the pores according to the IUPAC-isotherm. The average pore diameter was determined with the method of Barrett, Joyner and Halenda (BJH) and by the Kelvin equation. The total pore volume was obtained at 0.99 relative pressures. The samples were previously degassed out at 473 K for 3 h to remove water and CO_2.

Point zero charge pH (pH_{pzc}) and basicity and acidity surface functional groups determination

The pH_{pzc} was determined mixing 25 ml of 0.01 M NaCl solution with 75 mg of mineral samples at room temperature. The pH values were previously adjusted between 2 and 12, with intervals of 1 unit by adding 0.1 M HCl or NaOH solutions. After 24 h of contact, the samples were centrifuged, decanted, and pH was analyzed in the final liquid phases with a Conductronic pH 120 equipment.

Concentrations of the acid–base groups of materials were obtained as follows: for the basicity surface, samples of 200 mg of the materials were put in contact with 25 ml of a 0.025 M HCl solution and were placed in dark glass bottles and shaken for 24 h at 120 rpm at 303 K. After the samples were decanted, the excess of acid was titrated with 0.025 M NaOH. For the acid surface, a similar procedure was carried out, where a 0.025 M NaOH solution was put in contact with materials, and the titration solution was 0.025M HCl (Faria *et al*., 2004). The experiments were performed twice. The experiment was carried out for the three minerals separately.

Adsorption kinetics

The influence of the contact time over the amount of MG removal using BEN, TUF and VT minerals was studied to a dye initial concentration of 50 mg l^{-1}, adding 10 ml of dye solution to 10 mg of each mineral, separately. The mixture was shaken at different times (4, 6, 8, 10, 20, 30, 40, 50, 60, 70, 80, and 100 min) at 120 rpm and room temperature. After that, the samples were centrifuged and decanted. These experiments were performed in

duplicate.

Adsorption isotherms

10 mg of each mineral was put in contact with 10 ml of different initial concentration of dye (30-120 mg l^{-1}) with stirring during equilibrium time at room temperature. The mixture was centrifuged and decanted. The pH of each solution was measured before and after the treatments. The kinetic and adsorption data of the adsorbed amount of dye at time, qt (mg g^{-1} of adsorbent), were obtained by equation 1:

$$(C_o - C_t) \cdot V / m = q_t \qquad (1)$$

Where, Co (mg l^{-1}) is the initial dye concentration, Ct (mg l^{-1}) is the concentration of the solution at time t, V (l) is the volume of treated solution, and m (g) is the corresponding mass of BEN, TUF and VT minerals.

Colum adsorption experiment

The column dimensions were 16.0 cm of length and 1.0 cm of diameter. The flow rate was 5 ml min^{-1} the initial concentration of MG studied was 50 mg l^{-1} and 100 mg l^{-1}. All experiments were conducted to a constant temperature of 298 K.

Results and discussion

Characterization of minerals

Scanning Electron Microscopy

The three minerals possess an irregular texture formed by aggregation of particles of different sizes and forms being their morphologies similar among each other (Figure 2 a, b and c). The porosity of these materials is not detected due to the magnification employed to observe the specimens; the minerals porosities would be in the range of mesoporous materials (2 - 50 nm).

The elemental composition of these minerals by Energy Dispersive X-ray Spectroscopy (EDS) analyses, is shown in Table 1. Si, Al and O are identified as the main elements in BEN and VT minerals, and Ca, Si and O in TUF mineral, being characteristics of aluminosilicate minerals the presence of Si, Al and O elements. The amount of Ca in TUF indicates the main phase is rich in this element. The content of Si and Al on VT is in concordance to the composition of tuffs minerals reported [10].

Table 1. EDS analyses of BEN, TUF and VT minerals.

Elements	Weight percent (%)		
	BEN	TUF	VT
C	3.55±7.09	14.70±11.72	9.85±14.84
O	51.16±8.89	48.46±13.46	52.41±8,59
Na	-	0.01±0.04	0.17±0.37
Mg	0.74±0.52	0.12±0.27	0.73±0.61
Al	8.79±3.01	1.09±1.56	5.21±1.59
Si	23.62±8.60	9.97±8.51	26.74±10.36
Ca	8.95 ±1.01	25.18±21.58	1.03±0.64
Fe	1.46±9.67	0.47±0.76	2.86±1.42
K	-	-	0.90±0.89
Ti	1.73±3.51	-	0.10±0.47

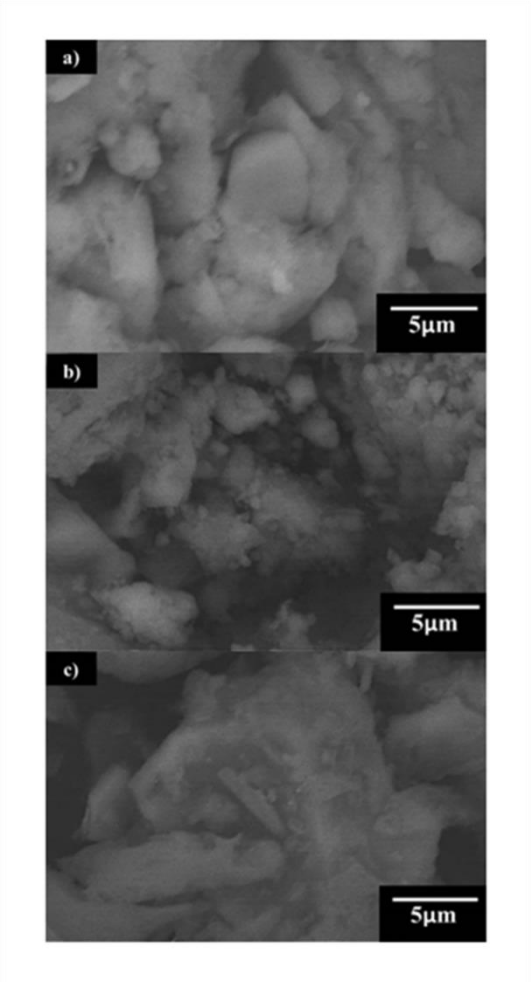

Figure 2. SEM images of BEN (a), TUF (b) and VT (c) minerals, BEC, 20 kV, x5000.

Chemical Composition-ICP

Chemical composition obtained by ICP technique indicated that the three minerals contain alkaline and alkaline-earths elements and transition metals

(table not shown), but the last ones in less proportion, with the exception of bentonite that exhibits more iron content, which agrees with EDS analysis.

BEN mineral has SiO_2 (56.24 %) and Al_2O_3 (22.58 %) mainly. This is a clay whose chemical composition is similar to others deposits located in several regions of the world (Kurniawan *et al*. 2012). BEN was originated from alteration of volcanic glass and/or tuffs and ash deposits like VT mineral (Blanco-Varela *et al*., 2006).

In TUF, CaO is the predominant compound, about 50%, followed by SiO_2 (17.71%). The high percentage of CaO in TUF suggests that the predominant phase in this mineral must be $CaCO_3$, since in Cuba calcite predominates as rock and is commonly found it in most deposits of minerals, either by contaminating them or being the principal phase, like in this case (Blanco-Varela *et al*., 2006).

The chemical compositions of VT mineral were reported previously (Blanco-Flores *et al*., 2014) where SiO_2 and Al_2O_3 represent almost the 80% of VT mineral composition. In general, the three minerals have a multicomponent character.

Infrared Spectroscopy

The IR spectrum of BEN (Figure 3a) shows broad absorption bands around 3500-3300 cm^{-1}, which can be attributed to stretching vibrations of structural –OH groups of bentonite. The band at 1637 cm^{-1} can be ascribed to angular deformation vibration of H-O-H in water within the interlayer space and the band at 3619 cm^{-1} to hydroxyl group bonded to Al^{3+} cation. The sharp and weak bands at 793 cm^{-1} and 680 cm^{-1} can be assigned to the presence of free silica and quartz, respectively. The Si-O vibrations are observed at 987 cm^{-1} and Al-Al-OH vibrations correspond with band to appear at 906 cm^{-1}. The bands around 500-400 cm^{-1} can be endorsed to Al-O-Si (octahedral Al) and Si-O-Si (tetrahedral Si) bending vibrations (Burcu and Özgür 2012).

TUF mineral IR spectrum (Figure 3b) show bands in the 1500-700 cm^{-1} region. These bands evidence the presence of CaCO3, confirming the material's main phase. Thompson *et al*., (2012) reported that carbonates have an intense band between1500–1400 cm^{-1} of asymmetric profile, whereas other of reduced intensity appears in the region between 877-680 cm^{-1}. The bands of TUF mineral at 1442 cm^{-1}, 1035 cm^{-1}, 877 cm^{-1} and 680 cm^{-1}, coincide with signals reported in the literature that correspond to calcium carbonate (Blanco-Varela *et al*., 2006). Besides, a band appears at 1093 cm^{-1} which corresponds to the Si-O bond.

In the IR spectrum of VT (Figure 3c), the bands at 3619 cm^{-1} and 3391 cm^{-1} could be attributed to surface –OH groups of Si-OH and molecular adsorbed water on the surface. A band at 1637 cm^{-1} can be related with bending mode of water molecule. The bands observed at 987 cm^{-1} and 909 cm^{-1} are attributed to Si-O vibrations. The absorption band at 785 cm^{-1} corresponds to Si-O-Al vibration and the band at about 680 cm^{-1} to Al-O vibration (Kabra *et al*., 2013).

X-Ray Powder Diffraction (XRD)

The XRD patterns for BEN (Figure 4a) indicate that the sample consisted predominantly of montmorillonite, quartz and kaolinite-montmorillonite. In this case, the presence of montmorillonite phase can be suitable for a cationic dye adsorption, since montmorillonite has a pH-dependent surfaces, high exchange capacity and different modes of aggregation (Erdal, 2009).

XRD analysis of TUF shows the sample contains calcite as the main crystalline phase and Ca-clinoptilolite in minor proportion (Figure 4b), which is in concordance with the results obtained by IR analyses, which suggests TUF is a mineral constituted by calcium carbonate, and the chemical composition analyses corroborate it. The presence of clinoptilolite is due to deposits localization of this mineral in many regions of country (Orozco and Rizo 1998).

Although is possible to observe some peaks, which correspond to mordenite and montmorillonite-bentonite, X-ray diffraction analysis indicates that VT is an amorphous mineral (Figure 4c). Blanco-Varela et al., (2006) indicated that the volcanic tuff rocks are essentially make up from of volcanic glass fragments with several degrees of devitrification, which can be more or less altered. Depending on the degree of alteration, the resulting minerals are classified as clays (montmorillonite), zeolites (mordenite or clinoptilolite) and so on.

BET Surface Area (S_{BET})

The amount of adsorbed nitrogen resulted to be higher in VT and BEN than in TUF (Figure 5), although the shape of isotherms is similar for the three materials. Adsorption isotherms are type IV, according to the IUPAC classification. Clear hysteresis loops are noticeable on the isotherms,

which indicate that the adsorption and desorption processes did not occurred in the same manner and the pores shapes are not uniform. The adsorption process on mesoporous solids is often accompanied by adsorption-desorption hysteresis, for this reason the appearance of isotherms is linked to mesopores in the samples. The shape of the hysteresis loops of each material corresponds with type H3. This type is characteristic of mesoporous solids; it is well known that type H3 hysteresis loops are associated with aggregates of plate-like particles giving rise to slit-shape pores (Kruk and Jaroniec, 2001).

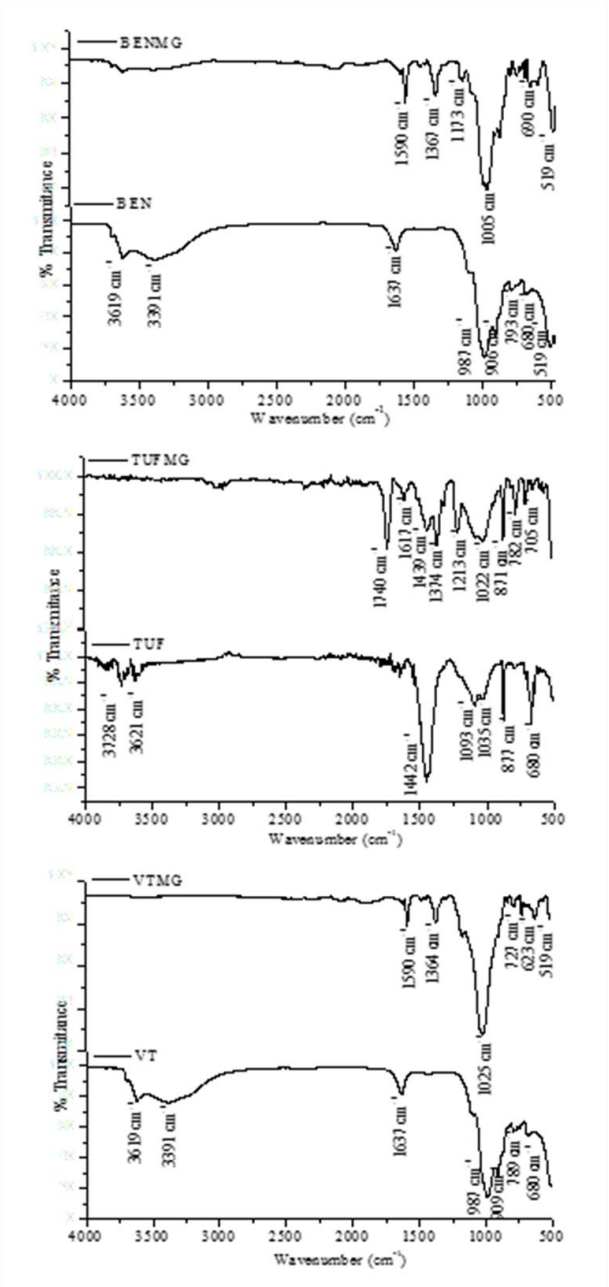

Figure 3. IR spectra before and after MG dye adsorption on BEN, TUF and VT minerals, respectively.

The higher difference in the hysteresis loops of the three materials is shown at the hysteresis loop width, which indicates that the pores shapes at BEN and VT materials are more irregular than TUF, where the adsorption pathway almost coincide with that of the desorption process, suggesting a similar or homogeneous porosity in TUF.

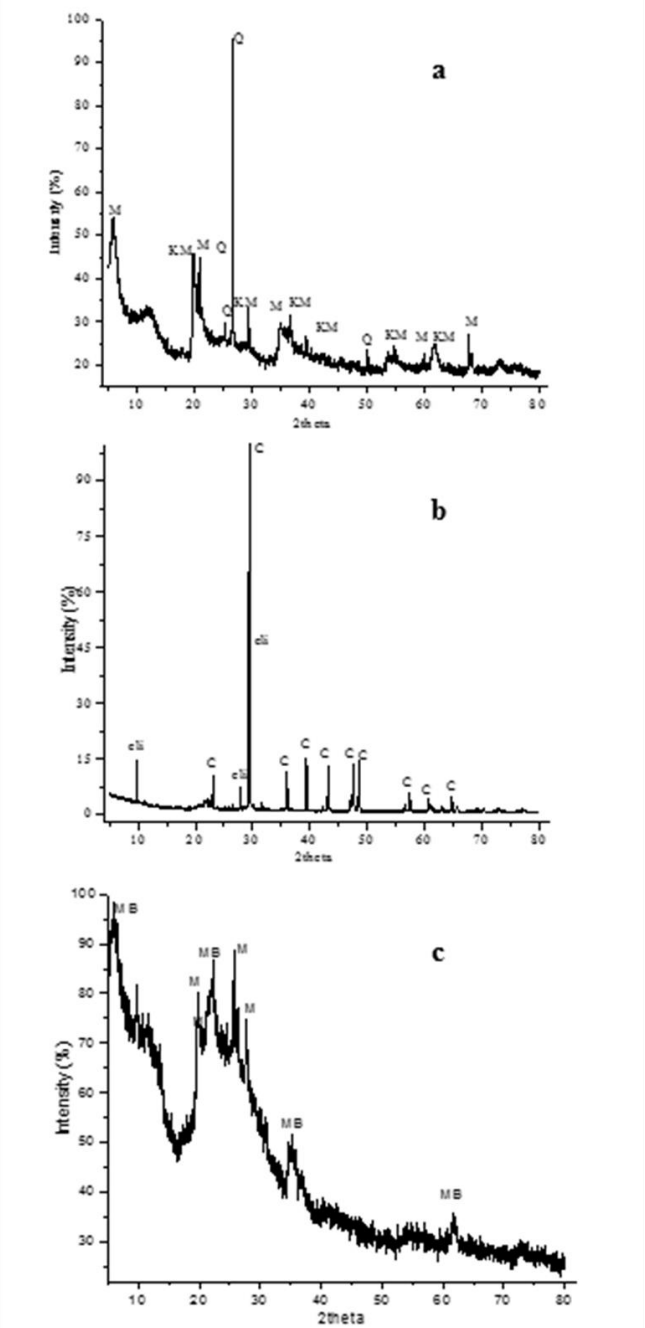

Figure 4. X-ray powder diffractograms of bentonite mineral (a: BEN, M: montmorillonite, Q: quartz, KM: Kaolinite-montmorillonite), tuff mineral (b: TUF, Cli: Ca-clinoptilolite and C: Calcite) and vitreous tuff mineral (c: VT, MB: montmorillonite-bentonite and M: mordenite).

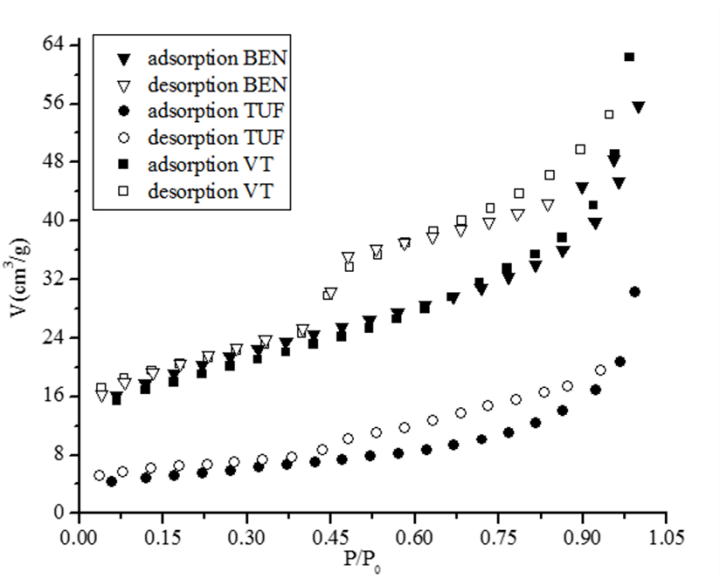

Figure 5. Adsorption-desorption nitrogen isotherm for BEN, TUF and VT minerals.

Adsorption-desorption isotherm for BEN and VT show an abrupt fall in the desorption path at P/P0 from 0.5 to 0.4. According to Kruk and Jaroniec (2001), this behavior is related with disorganized structure due to collapse of it. Also, BEN and VT minerals have more mesopores, close to the micropores range, than TUF, accordingly to the amount of nitrogen adsorbed at lower pressures. The total volume pore values, and the range of these values, indicate the presence of mesopores, agreeing to those published by Tsai *et al*., (2003). According to results, the surface area of these minerals is attributed mostly to mesopores (Sext), although the pores are narrow mesopores (Table 2).

In general, the minerals have small surface area compared to conventional adsorbent materials, such as activated carbon (Önal *et al*., 2006). If these surface area values achieved are compared to those obtained for minerals similar to BEN, TUF and VT, then the values of are somewhat larger (Acemioğlu, 2005; Toor and Bo, 2012; Boonyawan *et al*., 2010; Blanco-Flores *et al*., 2009).

pH_{pzc} and basicity-acidity surface groups determination

Surface chemistry of adsorbents is determined for the acid or basic character of it. The pH_{pzc} obtained for BEN clay was 8.66, this value is higher than other reported for a different type of bentonite (Vieira *et al*. 2010) because the presence of alkaline and alkaline-earths metals according to ICD and EDS analyses obtained. TUF material pH_{pzc} is 9.04; similar values of pH_{pzc}, 10.1 to 8.1 were reported for several types of calcite (Kosmulski, 2009). The pH_{pzc} for VT was 7.19. Silber *et al*. (2010) reported a value of 7.81 for perlite.

The difference between acidity and basicity values for BEN (Δ=54.9 m_{eq} g^{-1}) was lower than that in TUF mineral (Δ=141m_{eq} g^{-1}), this is because structure of BEN includes surface complexation sites, like silanol groups (Si-OH) and ion exchange sites (mainly alkaline and alkaline-earth elements). These results are in concordance with EDS and ICP results. However, for TUF mineral the higher difference agrees with its high calcium carbonate

Table 2. BET Surface area and total volume pore of the minerals

Mineral	S_{BET} (m^2 g^{-1})	S_{ext} (m^2 g^{-1})	S_{ext} (%)	S_{mic} (m^2 g^{-1})	S_{mic} (%)	V_t (cm^3 g^{-1})
BEN	69.1	57.7	83.5	11.3	16.4	0.080
TUF	18.4	16.9	91.6	1.8	9.8	0.045
VT	64.4	51.1	79.3	13.3	20.6	0.088

content, since this salt contributes to the basic character in aqueous medium.

Kinetic studies

The relationship between removal of MG dye and reaction time is reflected in Figure 6a. The equilibrium times for BEN, TUF and VT minerals are 55 min, 80 min and 60 min, respectively. In all cases, 94% removal of dye concentration is achieved before 30 minutes and then, the adsorption rates decrease until the equilibrium time is reached. According to Kumar *et al*., (2011) this trend is due to the adsorption dye onto the exterior surface of adsorbent at initial contact time. But considering

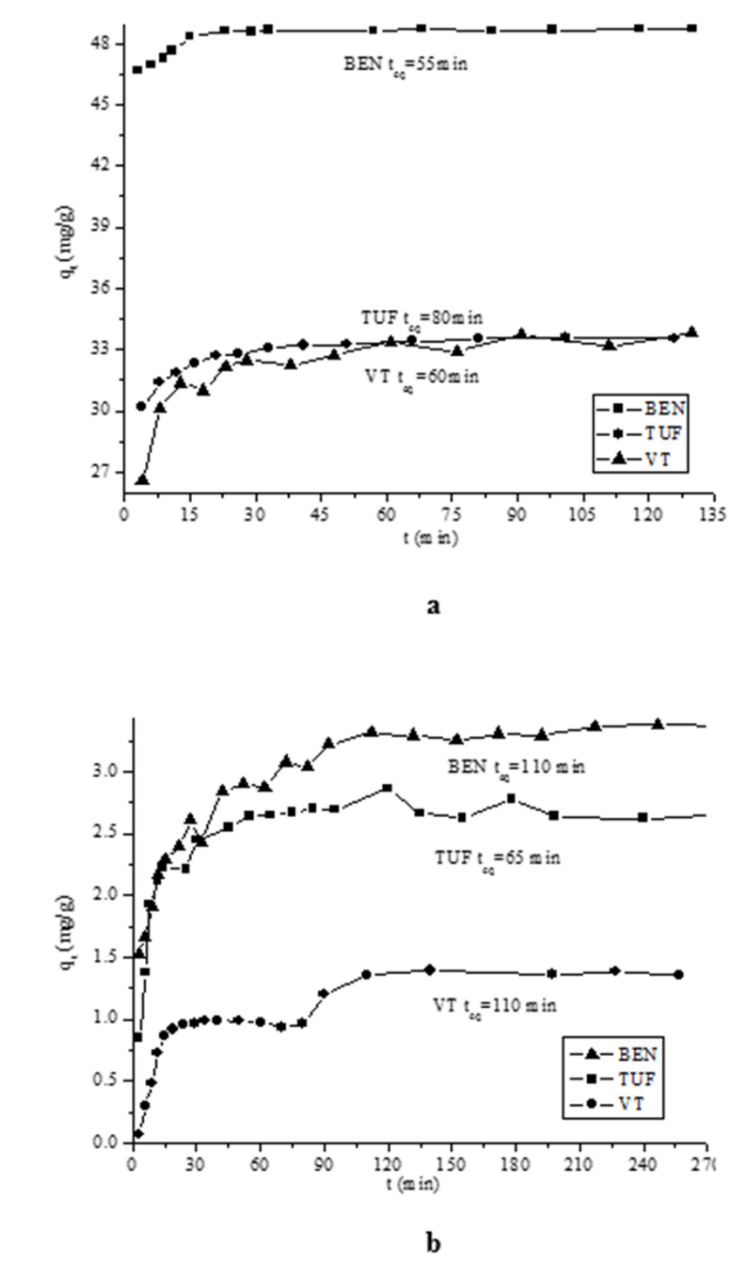

Figure 6. Kinetic adsorption of MG (a) and AG (b) dye on BEN, TUF and VT minerals.

that these minerals exhibit narrow mesopores, once the saturation point is reached, the adsorbate could diffuse into the less accessible pores in the interior surface of the adsorbent.

In order to elucidate the adsorption mechanism and the potential rate-controlling step, three kinetic models including pseudo-first-order, pseudo second-order, second order and intraparticle diffusion model (Ghaedi *et al*., 2014) were proved.

For the three minerals the values of residual sum of square (RSS) and reduced Chi-square are low for pseudo second order model compared with values of pseudo first and second order model and the values of correlation coefficient (R^2) is more close to the unit for former model than the latter one. Regarding the pseudo second order model, the values of adsorbed amounts of dye at equilibrium time, obtained experimentally (q_{exp}), and calculated values, (q_{cal}) are similar (Table 3). The results show good fitting to the three models; but the adsorption of MG dye in the three minerals is better described by pseudo-second order model, which may indicate that the sorption process is dominated by chemisorption.

When the intraparticle diffusion model is plotted for removal of MG by the minerals, a multilinearity having three linear zones is observed (Figure not shown). The lines of first zone did not pass through the origin suggesting that film diffusion and intraparticle diffusion occurred simultaneously in the three minerals. It seems that, the intraparticle diffusion controls the adsorption process rate in more extent. Thus, the period of zone II is higher than zone I. (Table 4).

The values of intercept C of intraparticle model provide information about the thickness of the boundary layer and the external mass transfer, this parameter decrease in the order BEN-TUF-VT, being the resistance to outer mass transfer higher that internal transfer in BEN mineral, this result is confirmed with film-diffusion and pore diffusion duration time.

The Boyd's model was applied to determine whether the main resistance to mass transfer is in the boundary layer or in the resistance to diffusion inside the pores (Lunhong *et al*., 2011). The Boyd

Table 3. Kinetics parameters for kinetic adsorption of MG and AG dye onto BEN, TUF and VT minerals.

Parameter	BEN		TUF		VT	
	MG q_{exp}=48.62	AG q_{exp}=3.29	MG q_{exp}=33.54	AG q_{exp}=2.64	MG q_{exp}=33.31	AG q_{exp}=1.35
Pseudo first order model						
q_{cal} (mg/g)	48.32	3.13	32.94	2.65	32.60	1.22
k_1 (min^{-1})	1.10	0.097	1.00	0.13	0.40	0.058
R^2	0.9979	0.8825	0.9950	0.9738	0.9897	0.8711
X^2	4.2717	0.0786	4.6651	0.0131	9.4356	0.0212
RSS	0.3286	1.6502	0.3888	0.2616	0.7863	0.4028
Pseudo second order model						
q_{cal} (mg/g)	48.71	3.36	33.55	2.80	33.64	1.40
k_2 (g/mg*min)	0.13	0.0448	0.06	0.0738	0.03	0.0483
R^2	0.9995	0.9633	0.9996	0.9739	0.9981	0.9130
X^2	1.0528	0.0246	0.4162	0.0123	1.7522	0.0143
RSS	0.0810	0.5160	0.0347	0.2592	0.1460	0.2719
Second order model						
a (mg/g)	$1.06 \cdot 10^9$	4.36	$6.23 \cdot 10^6$	10.39	$2.48 \cdot 10^5$	0.21
b (mg/g)	0.49	2.22	0.57	3.10	0.47	3.63
R^2	0.9786	0.9815	0.9893	0.8825	0.9898	0.9011
X^2	43.2618	0.0124	9.9078	0.0586	9.4119	0.0163
RSS	3.3278	0.2605	0.8257	1.1717	0.7843	0.3092

Table 4. Intraparticle diffusion model for adsorption of MG dye onto BEN, TUF and VT minerals.

Mineral	Film-diffusion		Intraparticle diffusion		
	time period (min)	k_1 (I) (mg $g^{-1} \cdot min^{0.5}$)	time period (min)	k_2 (II) (mg $g^{-1} \cdot min^{0.5}$)	C (II) (mg g^{-1})
BEN	0-15	0.277	15-33	0.033	48.13
TUF	0-16	0.34	21-51	0.038	32.35
VT	0-18	0.599	23-48	0.033	31.82

plots (Bt against time) do not pass through the origin and are not linear suggesting that film diffusion or chemical reaction control the adsorption rate.

Effect of dye structure on adsorption process

Analyzing the effect of dye structure, MG against AG, for BEN and VT minerals, the equilibrium time for kinetic process of AG dye (110 min for both) was higher than equilibrium time for kinetic process of MG dye (55 and 60 min respectively), almost twofold. However, for TUF mineral the equilibrium time was lower than the equilibrium time for kinetic process of MG dye. In all cases, the adsorption capacity equilibrium was lower for AG dye adsorption than for MG dye (Figure 6a and b).

Lower equilibrium times for MG than AG in kinetics adsorption may be caused by the molecular geometry, which is simpler for MG than for AG. The MG presents lower amount of functional groups in contrast to AG molecule (according to chemical structure, Figure 1 a and b). Analyzing the molecular mass of the two dyes (MMG=329.46 g mol^{-1} and MAG=622.57 g mol^{-1}), the MG could diffuse more rapidly through the minerals structure and the diffusive movement will be slower with AG. This idea corresponds with values of kinetics rate constant of the kinetics models applied (k_1 and k_2). An exception to this is the behavior of kinetics adsorption results found for TUF mineral.

The kinetics models were applied for AG dye adsorption, being the second order model that better described the process for BEN, the pseudo first order model for TUF and pseudo second order model for VT mineral. Therefore, each mineral interacts of different way with AG molecule. Therefore, it seems that the chemical affinity of dye by materials, geometry of dyes and functional groups in these organic compounds can affect the kinetic process.

Adsorption isotherms

The adsorption equilibrium of MG dye onto BEN, TUF and VT is obtained through adsorption isotherm (Figure not shown). Although there are many adsorption isotherms in the literature, the most widely used by researchers are two of the oldest isotherms, namely Freundlich, Langmuir and Langmuir-Freundlich isotherms (Gutiérrez-Segura *et al*., 2012), which are used in this study. The parameters of the isotherm equations used to describe the equilibrium adsorption nature are listed in Table 5.

The model that better fit to experimental data is Langmuir-Freundlich for the adsorption onto TUF and VT and Freundlich model when BEN mineral is used. These results suggest the adsorption process is better described by chemisorption of ionic dye onto heterogeneous surfaces, which agrees with the results obtained by SEM, chemical composition and the kinetic model that had better described the same adsorption process.

In all cases, the values of Freundlich parameter 1/n is less than 1 (1/n<1), these results indicate a favorable adsorption at this range of concentration. According to Venkat and Vijay (2011), the 1/n value indicates the relative distribution of energy sites and depends on the nature and strength of the adsorption process. For these cases, the 1/n values of three minerals refers to the fact that 66%, 28% and 24% of the active adsorption sites of TUF, VT and BEN minerals have equal energy and this can be related with chemical composition and centers of adsorption.

The maximum adsorption capacity of the adsorbent is the monolayer saturation at equilibrium and is increased in order: VT<BEN<TUF (71.22, 84.90 and 212.75 mg g^{-1}, respectively). The adsorption capacities obtained for the three minerals are in the range of the values that are reported to eliminate malachite green dye using different activated carbons (Almasi *et al*., 2016; Chinenye *et al*., 2016 and Ramya *et al*., 2016).

Table 5. Adsorption parameters of MG dye in BEN, TUF and VT minerals.

	Langmuir			Freundlich			Langmuir-Freundlich			
	q_{max} (mg g^{-1})	b (l mg^{-1})	R^2	K_F (mg g^{-1})(l mg^{-1})$^{1/n}$	1/n	R^2	K (mg g^{-1})	a (l mg^{-1})^n	1/n	R^2
BEN	84.90	0.75	0.9050	38.63	0.28	0.9372	37.30	0.037	0.27	0.9302
TUF	212.75	0.0099	0.9891	23.76	0.66	0.9899	23.14	0.057	0.8	0.9903
VT	71.22	1.06	0.9663	38.80	0.24	0.9245	76.74	1.23	0.02	0.9831

The IR spectroscopy spectrum of BEN mineral after the MG dye was adsorbed (BENMG) shows changes in the intensity and position of bands in comparison with the spectrum before MG adsorption (Figure 3a). The decrease of the intensity of bands assigned to –OH groups (3391 cm^{-1}) may indicate an interaction between dye and these groups, as well as the shift of the band at 1637 cm^{-1} to 1590 cm^{-1}, after adsorption. In addition, the change in the shape and intensities of bands in the 990-500 cm^{-1} region can indicate the modification of material due to dye adsorption. The signal characteristics of MG dye appear at 1367 cm^{-1}, 1173 cm^{-1} and 1005 cm^{-1} confirming MG adsorption onto BEN mineral. In contrast, the IR spectra of TUF material after MG adsorption (TUFMG) exhibit some important aspects (Figure 3b). The first is the decrease in the bands intensity corresponding to calcium carbonate. The second is the appearance of new bands related to functional groups of MG dye (1439 cm^{-1}, 1374 cm^{-1} 1213 cm^{-1} 1035 cm^{-1}, 782 cm^{-1} and 705 cm^{-1}). The third is the shifting of some mineral's bands of the main phase, when the dye is adsorbed and the last aspect is the showing of new bands (1617 cm^{-1} and 1740 cm^{-1}) maybe related with formation of new product due to interaction of malachite green with mineral or the occurrence of other removal process, such as precipitation. This idea is possible because the adsorption model that better fit to experimental data indicated that occurrence of simultaneous removal processes. To corroborate this, the TUF mineral was treated with acid solution (HCl 0.1 M), in this case the main phase disappear by a reaction of neutralization. The maximum adsorption capacity of dye onto treated mineral (TUFHCl, q_m=84.26 mg g^{-1}) was twice less for TUF, confirming the importance of $CaCO_3$ phase in the MG dye removal.

When MG dye was adsorbed by VT (VTMG), the bands at 3619 cm^{-1}, 3391 cm^{-1} and 909 cm^{-1} disappeared. In addition, the bands at 1364 cm^{-1} and 1025 cm^{-1} appeared and correspond to MG dye bands (Figure 3c). All this suggests the dye molecules can be interacting with mineral surface moities.

Adsorption of acid green 25 dye

The adsorption isotherm of AG dye onto BEN, TUF and VT, was analyzed using the same isotherm model above mentioned. In this case the maximum adsorption capacity was achieved in the order: VT>BEN>TUF (130.30 mg g^{-1}, 119.56 mg g^{-1} and 25.43 mg g^{-1} respectively). The behavior of the adsorbent mineral in the acid dye removal was different to that obtained for the basic dye.

Adsorption dye mechanisms

It seems that the dye can be removed from aqueous solution using a clay mineral by two pathways: first, surface exchange reactions, and second, through dye molecules diffusion into BEN layers for interactions and/or reactions such as ion-exchange, and complexation interactions Bulut *et al*., (2008).

In BEN case, according to kinetics results, the removal of MG was achieved through a combination process. Since the pH_{sln} after adsorption process (6.57-7.75) is lower than pH_{pzc} (8.66), the surface of bentonite is charged positively and the occurrence of a complexation reaction is less favorable because the MG is a cationic dye. For this reason, the dye removal can occur through ion exchange between positively charged groups in dye and alkaline or earth-alkaline ions initially present in the exchange position of the bentonite. The occurrence of two removal process is reasonable, taking in account that the clay exchange capacity (CEC=50.72 m_{eq} $100g^{-1}$) (Batista *et al*., 2010) is lower than the adsorption capacity of it (Figure 7a).

Roulia and Vassiliadis (2008) consider that usually clays absorb large amounts of dye cations (more than 100 % of the cation exchange capacity). This suggested, in our case, the formation of an organic-clay complex. The removal can also be promoted by interactions between π-electron systems of the conjugated aromatic dye with the surface of the clay.

The TUF mineral is rich in calcium carbonate, a substance that provides a basic character to the solution. The MG dye can be removed in basic condition through precipitation reaction. The dye can exist in three forms: chromatic malachite green, carbinol base and leuco malachite green. The dye shows a neutral carbinol base, which predominately exists above neutral pH. Taking in account the pH_{sln} values (7.44-8.20), for TUF mineral, the removal may occur through interaction between carbinol base MG dye and Ca^{2+}, also the precipitation reaction can occur due to the alkaline conditions (Young-Chul *et al*., 2013).

For TUF, the precipitation process occurs faster than adsorption process. When kinetics adsorption was realized for this mineral, the equilibrium time

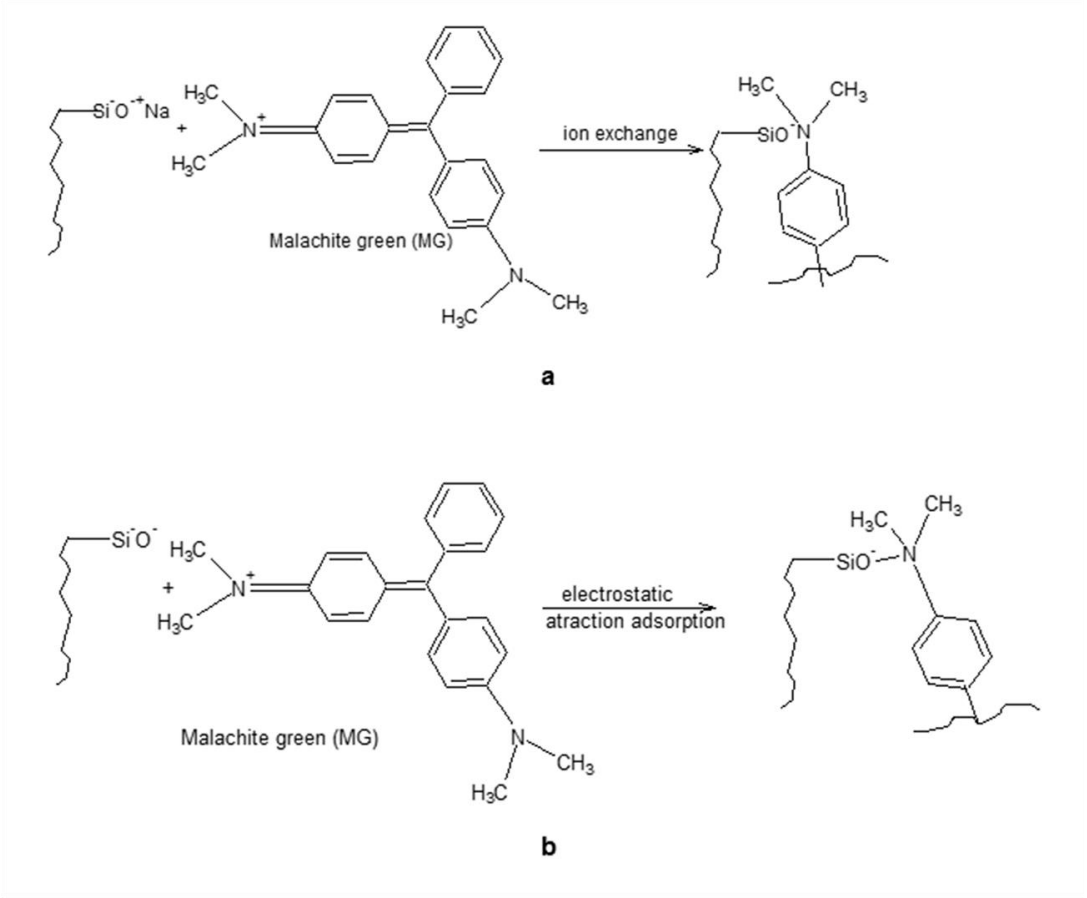

Figure 7. Schematic representation of suggested MG removal mechanism for BEN (a) and VT (b) minerals.

(teqTUF=80 min) was lower than the equilibrium time of washed with hydrochloric acid mineral (TUFHCl, t_{eq}TUFHCL=120 min) pointing out that without the presence of calcium carbonate the removal of dye is slow. This aspect together with the new bands appearance on FTIR spectrum of TUFVM (Figure 3b) suggested the occurrence of other process to removal MG dye, specifically the precipitation process.

The lower removal of dye by VT could be attributed to a geometric factor and the amount of silanol surface groups. The pH_{pzc} value (7.04) is lower than pH_{sln} (7.68-8.17) inferring the dye removal can occur through electrostatic interaction between the surface groups, identified by the IR spectra, and nitrogen atom of dye, charged positively (Figure 7b).

Perhaps the most important aspect in this investigation is the synergic effect found for TUF mineral. This mineral can remove a higher amount of dye and at the same time can increase the pH of the solution to basic values. This aspect is very interest because in most water treatment processes the pH is acid and is necessary to increase it to obtain a useful water for many applications such as: agriculture, industry and domestic and avoid corrosion. Besides, in water treatment use calcium carbonate is used as a precipitation agent and after that to perform other adsorption treatments. Using TUF mineral can avoid consumption of this chemical compound in water treatments.

Analyzing the behavior of AG dye adsorption, is probable the sylanol groups on surface of VT could interact with some functional groups of molecule structure such as $–SO_3$- through electrostatic attraction and hydrogen bond with –NH groups (Figure 1b). The first idea is supported by the fact that the pH of final solutions (pH_{sln}) was 6.50-6.63.

On the other hand, since pH_{zpc} was higher, then the surface material was positively charged and caused this interaction. BEN mineral can remove more amount of dye possibly by the presence of Si-OH groups and its exchange ions capacity. It surface was positively charged (pH_{sln}=7.43-7.60) as well as VT mineral. The electrostatic attraction also took place like another mechanism of dye molecules removal. Therefore, the BEN and VT minerals exhibited more affinity for acid dye than TUF, the last one presented more removal capacity for basic dye. The calcium carbonate present on TUF mineral do not favor the removal of acid dye, in contrast, the presence of silanol groups and exchange ions contribute to improve the adsorption. This could be related to the absence of –OH group in the dye molecule and its charge when it is dissolved in water.

Column study

The effect of initial MG dye concentration was investigated using TUF as adsorbent using column experiments. The breakthrough curves are shown in Figure 8. The breakthrough time (t_r) decreased with increasing dye concentration, besides the shaper of breakthrough curves change with increase of this parameter. Both aspect indicated the adsorption sites were occupied much faster when dye concentration increase.

In this study the experimental data was fitted with Bohart-Adams, Thomas and Yoon Nelson models, to determine the best model that describes the experimental results (Gutiérrez-Segura *et al*., 2012). The values of models parameters are shown in Table 6. Bohart-Adams and Thomas model better described the adsorption process for C_o=50 mg l^{-1} process.

The adsorption capacity from Thomas model was equals than the values obtained from equation 2, related to Yoon-Nelson model. According to Yoon-Nelson parameters the values of τ decreased when initial concentration increased due to the saturation of the column occurred more rapidly.

$$q_o = \frac{C_o \cdot Q \cdot \sigma}{m} \qquad (2)$$

For both experiments, the value of No and kAB decreased to initial concentration. It could be attributed to the contact time of dye solution with adsorbent was lower when initial concentration increased because the mass transfer zone decreased. Also the column could saturated more rapid to higher concentration. The same results were obtained with k_{TH} Thomas value because the process can be govern by extern mass transfer at the first time of column.

Comparing values of adsorption capacity for batch (q_o=212.75 mg g^{-1}), column system (q_{rea}l=20-50 %·$q_{Langmuir}$, q_{real}=42.4-106 mg g^{-1}) and Thomas values ($q_{oTH50mg\,l^{-1}}$=7.06 mg g^{-1} and $q_{oTH100mg\,l^{-1}}$=7.95

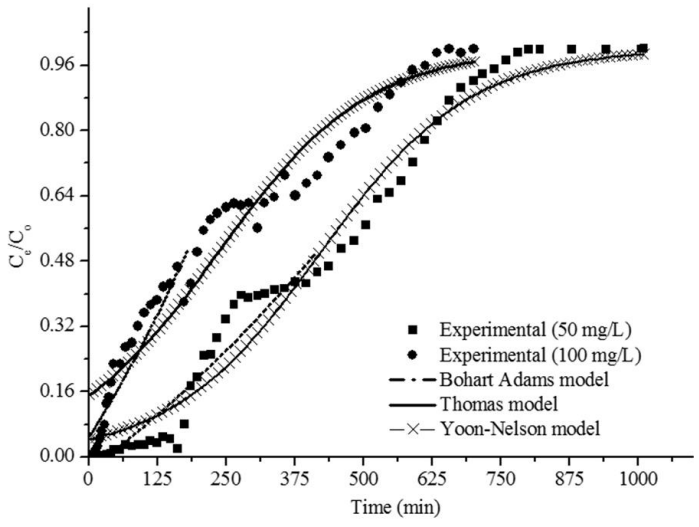

Figure 8. Effects of initial MG dye concentrations on the breakthrough curves using TUF as adsorbent.

mg g^{-1}), the mineral (TUF) may work better for a batch than column system. This behavior is because the adsorption column systems is a dynamic process, and if does not reach the equilibrium then the adsorption capacity decreases.

Conclusions

The present study demonstrated that BEN, TUF and VT minerals can be used as adsorbents for the removal of basic malachite green (MG) dye from aqueous solutions. These minerals are mesoporous materials and show different surface functional groups, all of them responsible of dye removal from aqueous solutions. The amount of dye removal was found to vary with increasing contact time. The kinetics of MG dye removal followed a pseudo second order kinetic expression for the three materials. The dye uptake process was found to be controlled by external mass transfer and intraparticle diffusion, but mainly for the former. The adsorption capacities obtained for VT, BEN and TUF were 71.22, 84.90 and 212.75 mg g^{-1}, respectively. Taking into consideration all the above obtained results, it can be concluded that these three minerals can be good alternatives as low-cost adsorbents for efficient dye removal in wastewater treatment processes; nonetheless, TUF resulted to be the best adsorbent material in batch systems. The experimental data using TUF in a column system were analyzed for two initial dye concentration and were fitted to three models. Based on these results, it is concluded that TUF mineral could be used as an effective adsorbent for malachite green dye removal from aqueous solutions.

Acknowledgments

We thank the financial support from PROMEP/103.5/13/6535 project, UAEM/2708/2013, and ABF is thankful to CONACYT for scholarship Grant No. 289993. We are indebted to MSc. Alejandra Núñez Pineda (elemental and IR analyses) and to MSc. Lizbeth Triana Cruz (IR analyses), both at CCIQS, UAEM-UNAM, for their technical support.

References

Acemioğlu, B. 2005. Batch kinetic study of sorption of methylene blue by perlite. Chemical Engineering Journal, 106: 73-81.

Almasi, A., Meghdad, P., Sohrab, A., Kiomars, S., Masoud, M., Yahya, J. 2016. Modeling and statistical analysis of malachite green dye removal from aqueous solutions by activated carbon powder prepared from Pine Bark (Modified by Sulfuric Acid)-Application of Response Surface Methodology. International Research Journal of Applied and Basic Sciences, 10: 5-12.

Arellano-Cárdenas, S., López-Cortez, S., Cornejo-Mazón, M., Mares-Gutiérrez, J.C. 2013. Study of malachite green adsorption by organically modified clay using a batch method. Applied Surface Science, 280: 74-78.

Batista, G. R., Coutin, D.P.C., González, C.D. Torres, Z.J.L. 2010. Valoración del potencial de las rocas y minerales industriales para el desarrollo municipal en la República de Cuba.

Blanco-Flores, A., Autie-Castro, G., Rodríguez-Montes, de Oca D., Paez, S.R., López-Cordero, R., Autie-Pérez, M. 2009. Características superficiales de un vidrio volcánico cubano y remoción de Cu2+ desde disoluciones acuosas. Revista Latinoamericana de Recursos Naturales, 5: 238-252.

Blanco-Flores, A., Colín-Cruz, A., Gutiérrez-Segura, E., Sánchez-Mendieta, V., Solís-Casados, D.A., Garrudo-Guirado, M.A., Batista-González, R. 2014. Efficient removal of crystal violet dye from aqueous solutions by vitreous tuff mineral. Environmental Technology, 35: 1508-1519.

Blanco-Varela, M.T., Martínez-Ramírez, S., Ereña, I., Gener, M. 2006. Pozzolanic reactivity of zeolitic rocks from two different Cuban deposits: Characterization of reaction products. Applied Clay Science, 32: 40-52.

Boonyawan, Y., Parncheewa, U., Buppa, P., Pawnprapa, K. 2010. Modification of calcite by hydration–dehydration method for heterogeneous biodiesel production process: The effects of water on properties and activity. Chemical Engineering Journal, 162: 135-141.

Bulut, E., Özacar, M., Şengil, I.A. 2008. Equilibrium and kinetic data and process design for adsorption of Congo Red onto bentonite. Journal of Hazardous Material, 154: 613-622.

Burcu, E.A., Özgür, A. 2012. The investigation of the effect of thermal treatment on bentonites from Turkey with Fourier transform infrared and solid state nuclear magnetic resonance spectroscopic methods. Spectrochimica Acta Part A, 94: 331-333.

Chinenye, A., Pius, C., Okechukwu, D., Ikenna, C. 2016. Adsorptive Treatment of Textile Wastewater Using Activated Carbon Produced from Mucuna pruriens Seed Shells. World Journal of Engineering and Technology, 4: 21-37.

El-Sayed, G.O. 2011. Removal of methylene blue and crystal violet from aqueous solutions by palm kernel fiber. Desalination, 272: 225-232.

Erdal, E. 2009. Removal of lead ions by Unye (Turkey) bentonite in iron and magnesium oxide-coated forms. Journal of Hazardous Material, 165: 63-70.

Faria, P.C.C., Órfão, J.J.M., Pereira, M.F.R. 2004. Adsorption of anionic and cationic dyes on activated carbons with different surface chemistries. Water Research, 38: 2043-2052.

Ghaedi, M., Ansari, A., Habibi, M.H., Asghari, A.R. 2014. Removal of malachite green from aqueous solution by zinc oxide nanoparticle loaded on activated carbon: Kinetics and isotherm study. Journal of Industrial Engineering Chemistry, 20: 17-28.

Gopinathan, R., Kanhere, J., Banerjee, J. 2015. Effect of malachite green toxicity on non-target soil organisms. Chemosphere, 120: 637-64.

Gupta, V.K.2009. Application of low-cost adsorbents for dye removal-A review. Journal of Environmental Management, 90: 2313-2342.

Gutiérrez-Segura, E., Solache-Ríos, M., Colín-Cruz, A., Fall, C. 2012. Adsorption of cadmium by Na and Fe modified zeolitic tuffs and carbonaceous material from pyrolyzed sewage sludge. Journal of Environmental Management, 97: 6-13.

Han, K., Sung-Oong, K., Sungyoul, P., Ho, S.P. 2015. Adsorption isotherms and kinetics of cationic and anionic dyes on three-dimensional reduced graphene oxide macrostructure. Journal of Industrial and Engineering Chemistry, 21: 191-1196.

Himanshu, P., Vashi, R.T. 2012. Fixed bed column adsorption of acid yellow 17 dye onto Tamarind seed power. Canadian Journal Chemical Engineering, 90: 180-185.

Kabra, S., Katara, S., Rani, A. 2013. Characterization and study of Turkish perlite. International Journal of Innovative Research in Science Engineering and Technology, 2: 4319-4325.

Kosmulski, M. 2009. pH-dependent surface charging and points of zero charge. IV. Update and new approach. Journal of Colloid and Interface Science, 337: 439-448.

Kruk, M., Jaroniec, M. 2001. Gas adsorption characterization of ordered organic-inorganic nanocomposite materials. Chemistry of Material, 13: 3169-3183.

Kumar, K.A., Gupta, N., Chattopadhyaya, M.C. 2011. Removal of cationic methylene blue and malachite green dyes from aqueous solution by waste materials of Daucus carota. Journal of Saudi Chemical Society, 18: 200-207.

Kurniawan, A., Hogiartha, S., Indraswati, N., Ismadji, S. 2012. Removal of basic dyes in binary system by adsorption using Rarasaponin-bentonite: Revisited of extended Langmuir model. Chemical Engineering Journal, 189: 264- 274.

Lunhong, A., Chunying, Z., Fang, L., Yao, W., Ming, L., Lanying, M., Jing, J. 2011. Removal of methylene blue from aqueous solution with magnetite loaded multi-wall carbon nanotube: Kinetic, isotherm and mechanism analysis. Journal of Hazardous Materials, 198: 282- 290.

McBride, J.H., Spencer, W.G., Faust, L.D., Nelson, T.S. 2012. A structural study of thermal tufas using ground-penetrating radar. Journal of Applied Geophysics, 81: 38-47.

Önal, Y., Akmil-Başar, C., Didem, E., Sarıcı-Özdemir, Ç., Depci, T. 2006. Adsorption kinetics of malachite green onto activated carbon prepared from Tunçbilek lignite. Journal of Hazardous Materials, B128: 150-157.

Orozco, G., Rizo, R. 1998. Depósitos de zeolitas naturales de Cuba. Acta geológica hispánica, 33: 335-349.

Qian, L., Qin-Yan, Y., Hong-Jian, S., Yuan, S., Bao-Yu, G. 2010. A comparative study on the properties, mechanisms and process designs for the adsorption of non-ionic or anionic dyes onto cationic-polymer/bentonite. Journal of Environmental Management, 91: 1601-1611.

Qiangshan, J., Linxia, F., Hongyan, L., Peng, L. 2011. Preparation of surface-vitrified micron sphere using perlite from Xinyang, China. Applied Clay Science, 53: 745-748.

Ramya, Vinayagam, M., Murugan, D., Lajapathirai, C., Saravanan, P., Sivasamy, A. 2016. Adsorption of Malachite Green onto Chemically Activated Carbon Prepared from Waste Biomass. International Journal of Innovative Research in Science, Engineering and Technology, 5: 115-123.

Roulia, M., Vassiliadis, A.A. 2008. Sorption characterization of a cationic dye retained by clays and perlite. Microporous Mesoporous Materials, 116: 732-740.

Sarı, A., Karaipekli, A., Alkan, C. 2009. Preparation, characterization and thermal properties of lauric acid/expanded perlite as novel form-stable composite phase change material. Chemical Engineering Journal, 155: 899-904.

Silber, A., Bar-Yosef, B., Levkovitch, I., Soryano, S. 2010. pH-Dependent surface properties of perlite: Effects of plant growth. Geoderma, 158: 275-281.

Thompson, P.S., Day, J.S., Parker, E.J., Evans, A., Chiu, T.C. 2012. Fine-grained amorphous calcium silicate $CaSiO_3$ from vacuum dried sol-gel-Production, characterization and thermal behavior. Journal Non-Crystalline Solids, 358: 885-892.

Toor, M., Bo, J. 2012. Adsorption characteristics, isotherm, kinetics, and diffusion of modified natural bentonite for removing diazo dye. Chemical Engineering Journal, 187: 79-88.

Tsai, W.T., Chen, H.P., Lai, C.W., Hsien, K.J., Lee, M.S., Yang, J.M. 2003. Preparation of adsorbents from sugarcane manufacturing by-product filter-mud by thermal activation. Journal of Analytical and Applied Pyrolysis, 70: 399-411.

Venkat, S., Vijay, B.P.V. 2011. Studies on the adsorption of Brilliant Green dye from aqueous solution onto low-cost NaOH treated saw dust. Desalination, 273: 321-329.

Vieira, M.G.A., Almeida, N.A.F., Gimenes, M.L., da Silva, M.G.C. 2010. Removal of nickel on Bofe bentonite calcined clay in porous bed. Journal of Hazardous Materials, 17: 109-118.

Xianming, M., Liping, L., Lin, C., Caiyun, S., Kwi, W., Shibao, Y., Jianguo, Z. 2012. Adsorption of heavy metal ions using hierarchical isotherm and kinetics studies. Journal of Hazardous Materials, 209: 467-477.

Young-Chul, L., Jin-Young, K., Hyun-Jae, S. 2013. Removal of malachite green (MG) from aqueous solutions by adsorption, precipitation, and alkaline fading using talc. Separation Science and Technology, 48: 1093-1101.